Three-dimensional generalized nonhyperbolic moveout approximation - 3D HTI model test

Qi Hao and Alexey Stovas, Norwegian University of Science and Technology*

Summary

We propose a 3D generalized nonhyperbolic moveout approximation to reflection traveltime. Thirteen parameters given in this approximation are determined by the zero-offset ray and two non-zero offset reference rays. We discuss three methods to exploit the traveltimes and their spatial derivatives in derivation of approximation parameters. A homogeneous 3D HTI model is used to test the accuracy of proposed approximation. Numerical results illustrate that accuracy of 3D generalized moveout approximation is model-dependent and influenced by the choice of reference rays. The potential applications of this approximation include velocity analysis, traveltime inversion etc.

Introduction

Reflection moveout approximation is important for time processing including velocity analysis, time migration etc. The 2D reflection traveltime as a function of source-receiver offset is generally nonhyperbolic in the vertically heterogeneous isotropic or homogeneous anisotropic overburdens. Numerous papers are devoted to study the moveout approximation for this case (e.g. Tsvankin 1994, 1995; Ursin and Stovas, 2006).

Two-dimensional traveltime approximation cannot satisfy the requirement of 3D seismic processing, since the azimuthal variation of reflection traveltime needs to be considered. Hyperbolic approximation of reflection traveltime is only valid for short-offset. NMO ellipse needs to be derived for hyperbolic approximation (e.g. Grechka and Tsvankin, 2002). Nonhyperbolic approximation becomes necessary for middle- and large-offset. Besides the NMO coefficients, the quartic moveout coefficients are required for the nonhyperoblic approximation (e.g. Pech and Tsvankin, 2003).

Fomel and Stovas (2010) proposed a 2D generalized moveout approximation (GMA) with good accuracy for a wide range of velocity models. The parameters for GMA of qP- and qSV-waves in 2D VTI media are defined in Stovas (2010). In this extended abstract, we extend their approximation to 3D case. The proposed approximation includes thirteen parameters to describe the azimuth variation of reflection traveltime from short to large offsets. Besides the zero-offset ray, two nonzero-offset rays with different azimuths are used to determine the parameters in 3D GMA. The accuracy of 3D GMA is tested on few 3D HTI models.

3D genearlized nohyperbolic moveout approximation

We extend the 2D GMA proposed by Fomel and Stovas (2010) to 3D case,

$$t^2(x,y) = (t_0^2 + a(x,y))(1-\xi) + \xi\sqrt{t_0^4 + 2t_0^2 b(x,y) + c(x,y)}\ , \tag{1}$$

$$a(x,y) = a_{xx}x^2 + 2a_{xy}xy + a_{yy}y^2\ , \tag{2}$$

$$b(x,y) = b_{xx}x^2 + 2b_{xy}xy + b_{yy}y^2\ , \tag{3}$$

$$c(x,y) = c_{xxxx}x^4 + 4c_{xxxy}x^3y + 6c_{xxyy}x^2y^2 + 4c_{xyyy}x^2y^2 + c_{yyyy}y^4\ . \tag{4}$$

From equations (1)-(4), we can see that 3D GMA have thirteen independent parameters including zero-offset traveltime t_0. Setting spatial coordinate x or y zero, 3D GMA can be reduced to 2D case.

Determination of parameters in 3D generalized moveout approximation

Zero-offset ray and two non-zero offset rays are selected to determine the thirteen parameters in equation (1). The Taylor expansion of traveltime squared at zero-offset ray is given by

$$t^2 = t_0^2 + W_{xx}x^2 + 2W_{xy}xy + W_{yy}y^2 + \frac{1}{2t_0^2}(A_{xxxx}x^4 + 4A_{xxxy}x^3y + 6A_{xxyy}x^2y^2 + 4A_{xyyy}xy^3 + A_{yyyy}y^4)\ , \tag{5}$$

where the coefficients W_{ij} define the NMO ellipse and coefficients A_{ijkl} are the quartic coefficients. Matching the coefficients of Taylor expansion of equation (1) to equation (5) up to 4th order, we obtain eight equations,

$$W_{xx} = (1-\xi)a_{xx} + \xi b_{xx}\ , \tag{6}$$

$$W_{xy} = (1-\xi)a_{xy} + \xi b_{xy}\ , \tag{7}$$

$$W_{yy} = (1-\xi)a_{yy} + \xi b_{yy}\ , \tag{8}$$

$$A_{xxxx} = \xi(c_{xxxx} - b_{xx}^2)\ , \tag{9}$$

$$A_{xxxy} = \xi(c_{xxxy} - b_{xx}b_{xy})\ , \tag{10}$$

$$A_{xxyy} = \xi\left(c_{xxyy} - \frac{2}{3}b_{xy}^2 - \frac{1}{3}b_{xx}b_{yy}\right)\ , \tag{11}$$

$$A_{xyyy} = \xi(c_{xyyy} - b_{xy}b_{yy}) \ , \tag{12}$$

$$A_{yyyy} = \xi(c_{yyyy} - b_{yy}^2) \ , \tag{13}$$

in addition to zero-offset traveltime t_0.

We introduce two non-zero offset rays by considering three different cases: For case I, we adopt the traveltime T and its derivative in y-direction $\partial_x T$ for one ray closed to x-axis, and traveltime T and its derivative in x-direction $\partial_x T$ for the other ray closed to y-axis. For case II, we use the traveltime and the sum of its partial derivatives $\partial_x T + \partial_y T$. For case III, we employ traveltime T , partial derivative $\partial_x T$ and $\partial_y T$ for two non-zero offset rays, respectively. For these cases mentioned above, we derive three basic equations from equations (1) and (9)-(13),

$$2F(x,y)b(x,y)\xi - (F^2(x,y) - 2t_0^2 F(x,y))\xi + A(x,y) = 0 \ , \tag{14}$$

$$\begin{aligned} &\partial_x F(x,y)b(x,y)\xi + F(x,y)\partial_x b(x,y)\xi \\ &+\partial_x F(x,y)\left(t_0^2 - F(x,y)\right)\xi + \frac{1}{2}\partial_x A(x,y) = 0 \end{aligned} \ , \tag{15}$$

$$\begin{aligned} &\partial_y F(x,y)b(x,y)\xi + F(x,y)\partial_y b(x,y)\xi \\ &+\partial_y F(x,y)\left(t_0^2 - F(x,y)\right)\xi + \frac{1}{2}\partial_y A(x,y) = 0 \end{aligned} \ , \tag{16}$$

where

$$F(x,y) = \frac{A(x,y)}{T^2(x,y) - t_0^2 - W(x,y)} \ , \tag{17}$$

$$W(x,y) = W_{xx}x^2 + 2W_{xy}xy + W_{yy}y^2 \ , \tag{18}$$

$$\begin{aligned} A(x,y) = &A_{xxxx}x^4 + 4A_{xxxy}x^3y + 6A_{xxyy}x^2y^2 \\ &+ 4A_{xyyy}x^2y^2 + A_{yyyy}y^4 \end{aligned} \ . \tag{19}$$

Equation (14) corresponds to the traveltime for a non-zero offset ray. Equations (15) and (16) can be derived by differentiating equation (14) with respect to x and y , which correspond to $\partial_x T$ and $\partial_y T$, respectively.

Substitutions of equation (3) to equation (14)-(16) result in three linear equations about four parameters ξb_{xx} , ξb_{xy} , ξb_{yy} and ξ for cases I and II. For case III, we obtain a linear system of six equations for these parameters. Singular value decomposition approach is used to estimate the least squares solution of this over-determined system. Once parameters b_{xx} , b_{xy} , b_{yy} and ξ are known, the eight parameters given in equations (2) and (4) can be determined from equations (6)-(13).

Parameterization of 3D HTI media

In our analysis, we focus on moveout of P-wave in acoustic approximation (Alkhalifah, 1998). The parameters of an acoustic VTI medium are: the vertical velocity of P-wave υ_0 , the NMO velocity $\upsilon_{nmo} = \upsilon_0\sqrt{1+2\delta}$ and anelliptical parameter $\eta = (\varepsilon - \delta)/(1+2\delta)$. For a 3D HTI medium, we have an additional parameter, the azimuth of the symmetry axis φ measured from x-axis.

For a horizontal reflector in 3D HTI media, we derive quadratic moveout coefficients,

$$W_{xx} = \frac{sin^2\varphi\upsilon_0^2 + (1+2\eta)^2 cos^2\varphi\upsilon_n^2}{(1+2\eta)\upsilon_0^2\upsilon_n^2} \ , \tag{20}$$

$$W_{xy} = \frac{sin(2\varphi)(-\upsilon_0^2 + (1+2\eta)^2\upsilon_n^2)}{2(1+2\eta)\upsilon_0^2\upsilon_n^2} \ , \tag{21}$$

$$W_{yy} = \frac{cos^2\varphi\upsilon_0^2 + (1+2\eta)^2 sin^2\varphi\upsilon_n^2}{(1+2\eta)\upsilon_0^2\upsilon_n^2} \ , \tag{22}$$

and quartic moveout coefficients,

$$A_{xxxx} = -\frac{4\eta(1+2\eta)^2 cos^4\varphi}{\upsilon_0^4} \ , \tag{23}$$

$$A_{xxxy} = -\frac{4\eta(1+2\eta)^2 cos^3\varphi sin\varphi}{\upsilon_0^4} \ , \tag{24}$$

$$A_{xxyy} = -\frac{\eta(1+2\eta)^2 sin^2(2\varphi)}{\upsilon_0^4} \ , \tag{25}$$

$$A_{xyyy} = -\frac{4\eta(1+2\eta)^2 cos\varphi sin^3\varphi}{\upsilon_0^4} \ , \tag{26}$$

$$A_{yyyy} = -\frac{4\eta(1+2\eta)^2 sin^4(\varphi)}{\upsilon_0^4} \ . \tag{27}$$

Numerical Examples

To analyze the influences of reference rays and HTI symmetry axis on the accuracy of 3D GMA for three cases mentioned above, we design several homogeneous 3D HTI models with a horizontal reflector. The model parameters are $z = 1km$, $\upsilon_0 = 2km/s$, $\delta = 0.1$, $\eta = 0.2$, $t_0 = 2z/(\upsilon_n\sqrt{1+2\eta}) \approx 1.543s$.

First, we choose two reference rays with same radial offset of $4km$. Figures 1 to 3 show the influence of the azimuth of HTI symmetry axis on absolute relative error in traveltime of 3D GMA (1) for cases I, II, and III, respectively. Due to the symmetric property of traveltime for azimuths of HTI symmetry axis equal to 0 and $\pi/2$, $\pi/6$ and $\pi/3$, we show only the plots for azimuth of HTI symmetry axis equal or less than $\pi/4$. For three cases, we can see that 3D GMA has relatively high accuracy when HTI symmetry axis is far away from the reference rays. The accuracy of 3D GMA firstly goes down then up with increase of the azimuth of HTI symmetry axis. 3D GMA has lowest accuracy when the azimuth of HTI symmetry axis reaches $\pi/4$, since the linear system constructed by equations (14)-(16) becomes poor-conditioned.

Next, we change the radial offset of the reference ray with the acquisition azimuth $\pi/12$ from $4km$ to $2km$. By comparing Figures 1 to 3 with Figures 4 to 6, we can see that modification of the offset of reference ray results in significant accuracy variation of 3D GMA when the HTI symmetry axis is closed to the modified reference ray.

From Figures 1 to 6, we can observe that all three cases are model-dependent, and case III has the best accuracy. This is due to the well-condition of the linear system constructed by equations (14)-(16), which increases the reliability of parameters determination for 3D GMA.

Conclusions

We propose a three dimensional generalized nonhyperbolic moveout approximation involving thirteen parameters. Only three rays are employed to determine these parameters, one zero-offset ray and two additional nonzero-offset rays. HTI model test confirms that the accuracy of our approximation is model-dependent. Both the azimuth of HTI symmetry axis and the offset of reference ray can affect the accuracy of our approximation significantly. The accuracy of our approximation can be improved by constructing an over-determined system to compute the required parameters.

Acknowledgement

We would like to acknowledge the ROSE project for financial support.

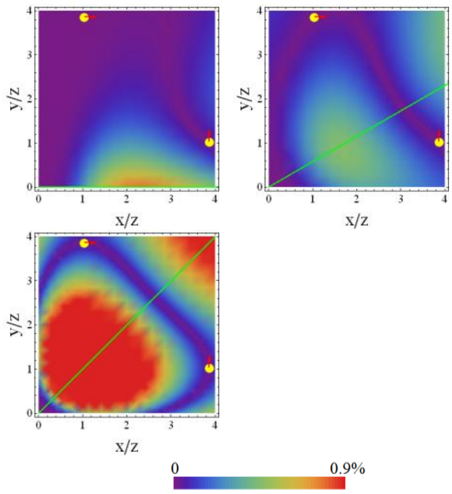

Figure 1. The influence of the azimuth of HTI symmetry axis on absolute relative error in reflection traveltime for case I. From top-left to bottom-left, the plots correspond to the azimuths of symmetry axis equal to 0, $\pi/6$ and $\pi/4$, respectively. The yellow points denote the positions of the reference rays. Green line denotes the azimuth of HTI symmetry axis. The red arrow shows the direction of traveltime spatial derivative.

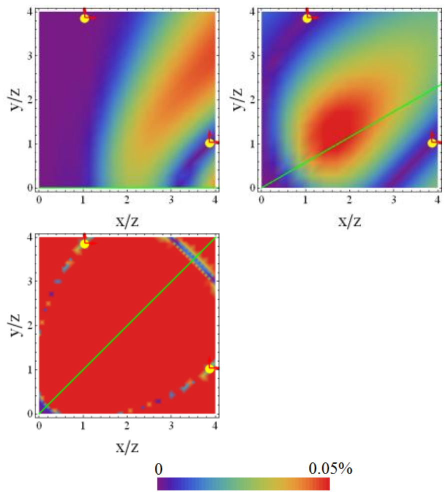

Figure 2. Similar to Figure 1, but for case II.

References

Alkhalifah T. 1998. Acoustic approximations for seismic processing in transversely isotropic media: Geophysics **63**, 623–631.

Fomel S., and A. Stovas, 2010, Generalized nonhyperbolic moveout apprimation: Geophysics, **75**, U9-U18.

Grechka V., and I. Tsvankin, 2002, NMO-velocity surfaces and Dix-type formulas in anisotropic heterogeneous media: Geophysics, **67**, 939-951.

Pech A., and I. Tsvankin, 2003, Quartic moveout coefficents: 3D description and application to tilted TI media: Geophysics, **68**, 1600-1610.

Stovas, A., 2010, Generalized moveout approximation for qP- and qSV waves in a homogeneous transversely isotropic medium: Geophysics, **75**, D79-D84.

Tsvankin I., and L. Thomsen, 1994, Nonhyperbolic reflection moveout in anisotropic media: Geophysics, **59**, 1290-1304.

Tsvankin I., 1995, Normal moveout from dipping reflectors in anisotropic media: Geophysics, **60**, 268-284.

Ursin B., and A. Stovas, 2006, Traveltime approximations for a layered transversely isotropic medium: Geophysics, **71**, D23-D33.

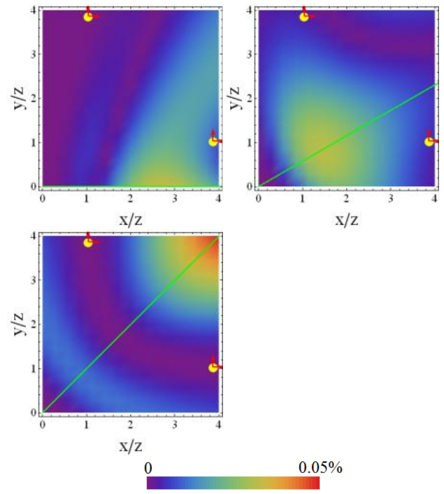

Figure 3. Similar to Figure 1, but for case III.

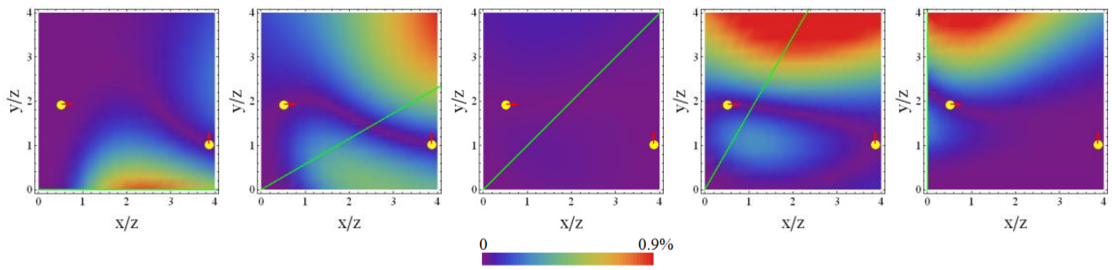

Figure 4. Similar to Figure 1 for case I, but with a shorter radial offset for one reference ray with azimuth of $5\pi/12$. From left to right, the azimuths of HTI symmetry axis are 0, $\pi/6$, $\pi/4$, $\pi/3$ and $\pi/2$, respectively.

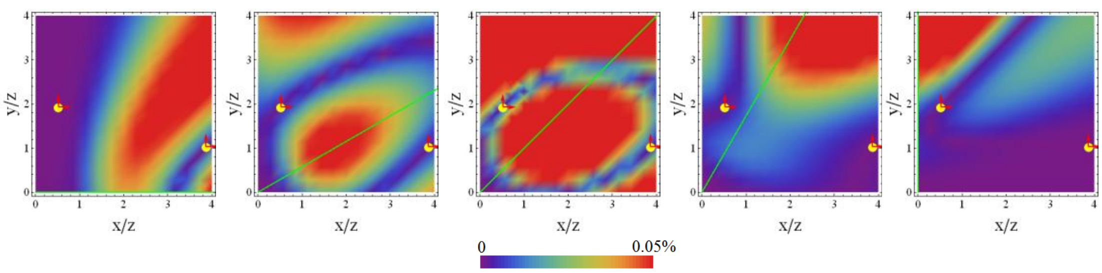

Figure 5. Similar to Figure 4, but for case II.

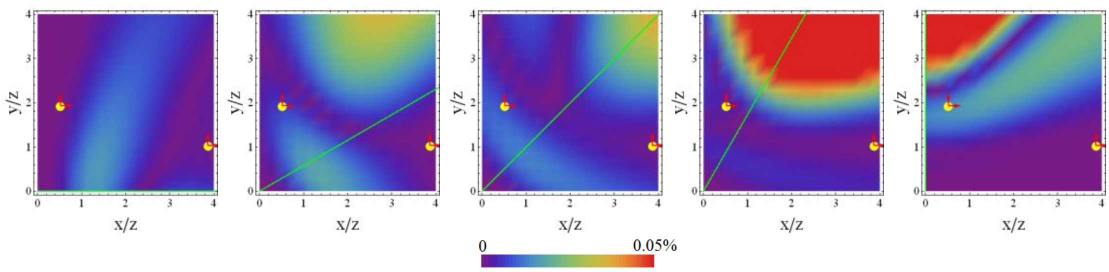

Figure 6. Similar to Figure 4, but for case III.